JOURNAL OF MATERIALS SCIENCE 30 (1995) 6028–6034

# Electron irradiation and microstructure in polypyrrole

C. D. G. MINTO, A. S. VAUGHAN*
*J. J. Thomson Physical Laboratory, University of Reading, P.O. Box 220, Whiteknights, Reading RG6 2AF, UK*

Free-standing films of polypyrrole have been electrochemically synthesized from solutions of pyrrole and *p*-toluene sulphonate in water. The resulting polymer was exposed to a variety of electron-beam conditions in an analytical scanning transmission electron microscope and the interaction between the electron beam and the sample was investigated by elemental X-ray spectroscopy and electron diffraction. In transmission mode, with an 80 kV beam, the films were found to be stable with respect to the production of sulphur X-rays for up to 500 live seconds. Molecular ordering was observed to be destroyed by the action of the beam. Such techniques, together with X-ray scattering, were subsequently utilized to examine spatial variations in molecular trajectory and counter-ion content; these variations were found to be associated with the nodular surface structure that characterizes polypyrrole.

## 1. Introduction

As techniques for the examination of polymeric microstructures, both transmission (TEM) and scanning electron microscopy (SEM) are well established. The electron microscope has been successfully used to examine and elucidate the microstructure of many crystalline and amorphous materials. The importance of microstructure and the usage of the electron microscope as a tool has clearly been revealed by work such as that by Bassett [1] and Tsuji [2]. It is, however, evident that direct exposure of polymers to the electron beam can induce artefacts in the specimen and such exposure can result in changes in crystallinity leading to complete loss of order within a short period of time. Grubb, for example, has shown [3] that degradation of the diffraction pattern of solution-grown polyethylene crystals is accomplished rapidly, the crystals retaining their shape but losing Bragg contrast; he goes on to describe mass loss and localized heating in such systems. Similarly, mass transport can lead to the "development" of structural features which are not initially visible, loss of contrast and sample thinning [4]. As a result, many studies (such as those by Vesely *et al.* [5]) have been executed to measure such effects in most common polymeric materials. Because the electron beam can clearly interact destructively with many polymer systems, it is prudent to quantify such effects in a given system, before any extensive direct analysis of the microstructure via transmission electron microscopy.

Conjugated conducting polymers are systems where the microstructure is of prime importance [6]; varying the sample treatments or growth conditions can radically alter the form and conductive properties of the material. For example, post-formation stretching in polypyrrole, amongst others, results in chain alignment and improved conductivity [7]; changing the synthesis parameters for many of these materials (e.g. polyaniline) can markedly alter the growth mechanism and the resulting morphology [8].

Polypyrrole is such a system and, consequently, many surveys of the surface morphology and structural anisotropy of electrochemically grown films have been undertaken [9–12]. Few attempts have been made to study the internal organization by transmission electron microscopy, but it is thought that this system is particularly prone to beam damage [13]. Before directly analysing the internal morphology, a knowledge of how the films react to the electron beam is, therefore, essential.

In the study described here, we have examined the stability of thin sections of electrochemically polymerized films of polypyrrole *p*-toluene sulphonate with respect to an electron beam, using a combination of (scanning) transmission electron microscopy, (S) TEM, and energy dispersive X-ray spectroscopy (EDS). By exposing sections to a variety of constant beam conditions and monitoring the resulting emissions, the effect of the interaction between beam and sample can be readily monitored and compositional changes quantified.

Films of polypyrrole can exhibit considerable anisotropy in the growth plane when examined by wide-angle X-ray scattering (WAXS) [9, 14]. Strong birefringence is also evident when this material is viewed between crossed polars in an optical microscope [15]. Although considered an amorphous polymer, polypyrrole is clearly imbued with some molecular ordering. The effects of electron irradiation on molecular packing and film anisotropy, were subject to examination on

* Author to whom all correspondence should be addressed.



0022–2461 

the macroscopic and microscopic levels by polarized optical microscopy and electron diffraction. The dominant molecular trajectory in films synthesized using the planar toluene sulphonate counter ion, is parallel to the growth electrode; however, it is not clear how this is disturbed by the non-planar radiating nodular and conical structures which characterize polypyrrole.

Knowledge of how such films react when exposed to an electron beam allows a full examination of the internal microstructure, utilizing techniques which may require the residence of a beam on a selected area for a considerable period of time. Such techniques have been employed to examine spatial variations in the composition. These are complemented with an investigation into molecular ordering within the films, via electron and wide-angle X-ray diffraction. Together, these techniques give a clear insight into the structure of polypyrrole.

## 2. Experimental procedure

### 2.1. Materials

The films of polypyrrole *p*-toluene sulphonate used in this study were prepared in a one-step electrochemical oxidative polymerization process. As the procedure is described in detail elsewhere [9], only an outline description follows; the procedure is similar to that applied by Diaz *et al.* [16]. Appropriate quantities of the pyrrole monomer and *p*-toluene sulphonate were dissolved in distilled water and the resulting solution placed in a three-compartment electrochemical cell. A Sycopel Model 801 potentiostat was used, operating under computer control, maintaining a constant voltage of 1.2 V (versus a saturated calomel reference electrode) at the working electrode (ITO coated glass). A carbon rod was used as the counter electrode. The procedure was carried out until a charge of between 6 and 24 C had passed through the cell, after which time the free-standing films, $\sim 10$ μm thick, were removed from the electrode surface, washed in distilled water and finally dried under dynamic vacuum.

### 2.2. Instruments and sample preparation

Specimens for microscopy were first embedded in Transmit EM, a four-stage low-viscosity epoxy resin supplied by TAAB Laboratories. The optimum mixture for sectioning the polypyrrole film was found to be of soft to medium hardness consisting of 26% EM resin, 37% of each hardener, TH1 and TH2 (all percentages by weight) and a 2% (weight/volume) of accelerator. The resulting resin mixture was cast into gelatin capsules containing supported sections of the synthesized films. The resin was cured at 70 °C for 16 h.

Ultra-microtomy was performed at room temperature using an RMC MT7 ultra-microtome. Samples were sectioned at 100 nm and chosen according to their interference colour in reflected light (silver and gold colours providing the optimum contrast). The samples were picked up on hexagonal copper grids (200 mesh size) and dried in air. On the basis of previous results [15], this method does not result in appreciable sample deformation and any observed anisotropy is therefore genuine.

The sections were examined using a Philips CM20 scanning transmission electron microscope; a double-tilt beryllium holder was used. X-ray analysis was carried out using an EDAX PV9900 energy dispersive analyser operating in both area collection and line scanning mode. The energy peaks from the sulphur ($SK_\alpha$) in the counter ion, the background fluorescence from the copper grid ($CuK_\alpha$) and an arbitrary count from the *bremstrahlung* background (taken at 1.54 keV) were monitored for the various experiments. The microscope was operated at 80 kV with a nominal spot size of 27.5 nm. A condenser aperture of 200 μm was selected and the magnification was chosen in order that the image of the film would fill the centre of the viewing screen (at a magnification of $\times 7800$). These settings produced a total count of $\sim 1000$ over 500 live seconds.

Wide-angle X-ray scattering measurements were performed on a Philips PW1120/90 X-ray generator, using pinhole collimated, monochromatized $CuK_\alpha$ radiation ($\lambda = 0.15418$ nm). The *d* spacings were calibrated against silicon powder which produces a characteristic Bragg reflection at 28.46°.

A Zeiss GFL polarizing microscope was used to examine specimen birefringence.

## 3. Results and Discussion

### 3.1. Irradiation and film composition

As described above, irradiation of polymers generally results in mass transport combined with a progressive loss of molecular ordering. In considering the effects of exposing polypyrrole to the electron beam in a TEM, three factors must therefore be considered.

(i) Irradiation may result in mass loss or sample thinning, but with no change in composition. All of the constituent components are affected equally by the beam.

(ii) The electron beam may affect one part (of what is essentially a two-component system – the counter ions and the polymer molecules) to a greater extent, such that irradiation results in a progressive change in composition.

(iii) Molecular ordering may be disrupted.

In considering these factors, two different methods were chosen to irradiate the sample. By defocusing the beam, the entire cross-section of the sample could be irradiated (area $\sim 120\ \mu m^2$). In addition, some measurements were also made using a focused spot ($\sim 30$ nm diameter).

Initially, the sample was exposed to the beam and at regular intervals the total count for the sulphur peak was monitored to give a record of the continuous output of characteristic X-rays for the region being analysed.

The results in Fig. 1 show the variation in the $SK_\alpha$ peak height over 500 (live) seconds for a film grown to 24 C. For both beam types, the behaviour is essentially linear. The trace from the defocused beam rises with a gradient of $\sim 133$ counts $min^{-1}$, whereas that from the focused beam is $\sim 164$ counts $min^{-1}$ (both values

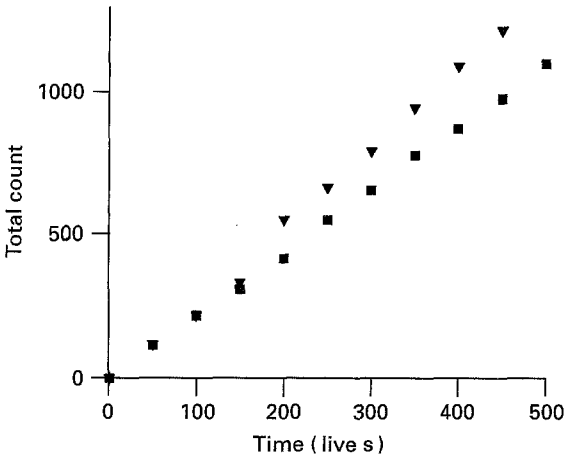


*Figure 1* Variation in total sulphur count with exposure time up to 500 (live) s for a (■) defocused (120 μm²) and (▼) focused (27.5 nm spot) 80 kV beam.

are for gradients evaluated over the last 200 s of the experiment). Up to 200 s the focused and defocused beams are essentially co-linear, after this the focused beam jumps slightly but then continues with the same gradient. Presumably this slight change is due to sample drift on to a sulphur-rich area, or some instability in the beam. The production rate of X-rays for the focused beam is slightly greater than that for the defocused beam, presumably because the area chosen for irradiation is rich in sulphur (see later). The linear nature of the response evident in Fig. 1 clearly demonstrates that little mass loss occurs during irradiation.

A defocused beam was then used to irradiate the specimen repeatedly for periods of 50 live seconds. Fig. 2a shows the variation in the $SK_\alpha$:$CuK_\alpha$ peak area ratio with irradiation time (after background subtraction). The magnitude of the $CuK_\alpha$ peak (due to the fluoresence) would be expected to stay constant for similar exposures, provided the sample is not being thinned by the electron beam. Because Fig. 1 indicates that extensive sample mass loss does not occur, this feature provides a useful reference. The response varies but the trend is essentially linear, so there is little degradation in the S signal. In Fig. 2b, the experiment has been repeated, but here, the sulphur output is compared to a count form an arbitrary background window (1.54 keV). As can be seen, the trace varies widely and there is some evidence of a trend towards a decrease in the sulphur counts with respect to the background, but this is in no way conclusive. It should be noted that the sample background is less than 10% of the peak height and thus comparatively large changes in the size of the background can be effected with a small number of counts, so altering the relative ratios.

It is evident from Figs 1 and 2 that exposing the sections to an 80 kV beam of electrons for up to 500 live seconds produces no evidence of mass loss or changes in chemical composition. This exposure provides a total count of over 1000 which is more than adequate for any experiment that could reasonably be contemplated.

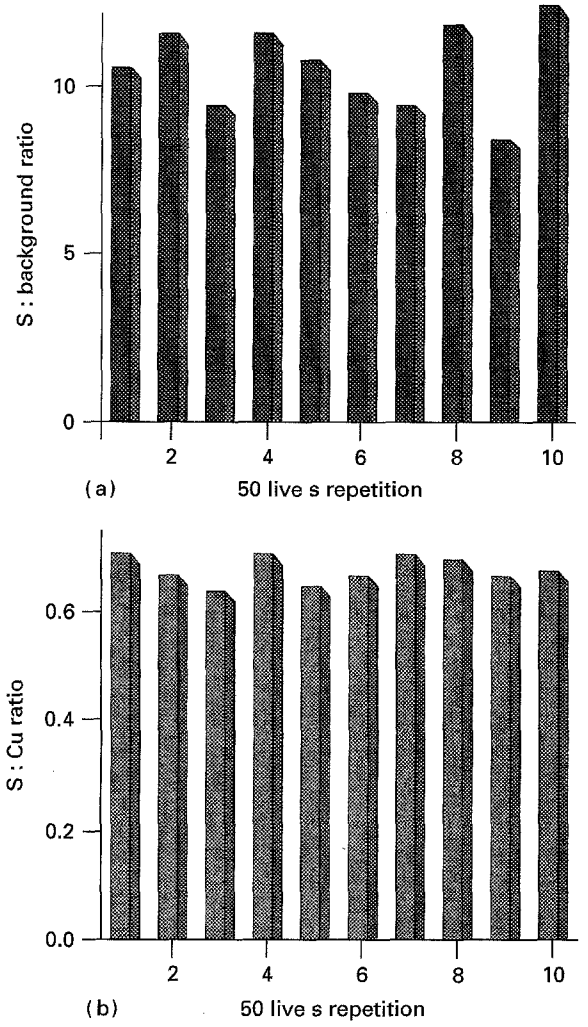


*Figure 2* Integrated peak area ratios for (a) $SK_\alpha$ to $CuK_\alpha$ and (b) $SK_\alpha$ to low background, for repeated 50 s exposure to a defocused 80 kV electron beam.

## 3.2. Irradiation and molecular anisotropy

Although polypyrrole is known to be non-crystalline, a degree of molecular ordering has been detected via WAXS of films in cross-section. In particular, the results gathered by Mitchell *et al.* [17, 18] demonstrate that the pyrrole rings are preferentially oriented parallel to the plane of the film. Optical observations [15] also reveal evidence of extensive molecular ordering in films viewed in cross-section. This anisotropy can also be detected readily via electron diffraction; a characteristic appearance such as that in Fig. 3, clearly exhibits quite strong anisotropy for an "amorphous" polymer. The reflections, which have been characterized with the pattern oriented as for a fibre pattern, are listed in Table I. Although these strong reflections are observed, they are purely based on planar ordering. The molecular trajectory is believed to be completely randomized within the plane of the film, such that any crystallographic interpretation is inappropriate. Nevertheless, it is evident that both the meridional and equatorial reflections appear periodic, the spacings being 0.45 and 0.33 nm (strongest reflection), respectively. Mitchell and Geri [14], using WAXS, found scattering peaks of $s \sim 20$ nm and $\sim 15\ nm^{-1}$ which gives interatomic spacings of $d = 0.31$ and

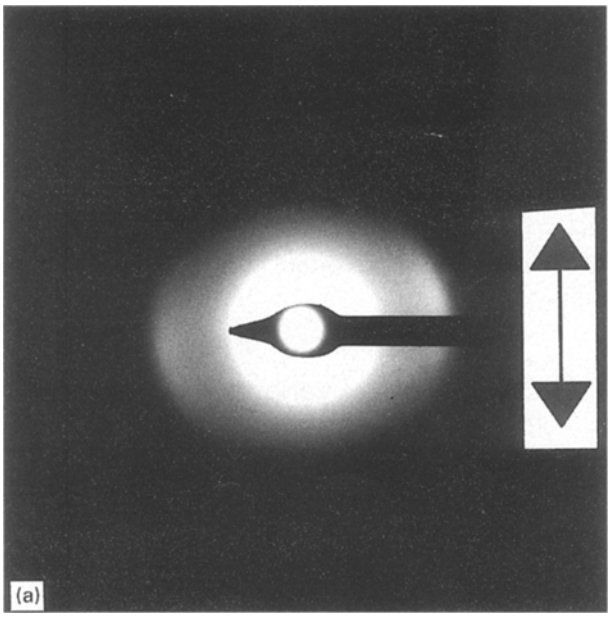


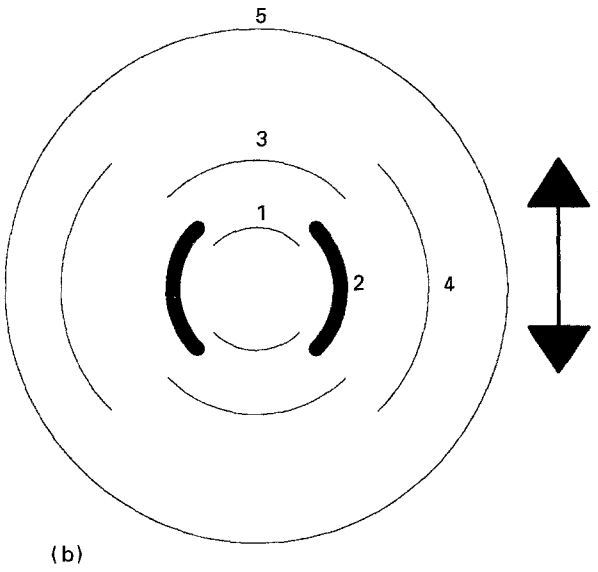


*Figure 3* (a) The electron diffraction of a pristine sample clearly showing the inherent ordering. (b) Schematic representation of the diffraction pattern showing all the detectable reflections. The arrow indicates the plane of the film.

TABLE I Interplanar spacings, visually estimated intensities and orientations for the observed polypyrrole reflections

| Reflection | $d$ (nm) | Intensity | Orientation |
|---|---|---|---|
| 1 | 0.45 | vw | Meridional |
| 2 | 0.33 | vs | Equatorial |
| 3 | 0.22 | s | Meridional |
| 4 | 0.16 | m | Equatorial |
| 5 | 0.11 | w | Meridional |

0.42 nm. These correspond well with the values quoted above. These $d$ spacings are also in excellent agreement with those reported by Geiss [19], although there no reference is made to our weak 0.45 nm reflection. The azimuthal angular spread from the strongest reflection is ~60°, clearly indicating that although orientation exists, it is far from perfect.

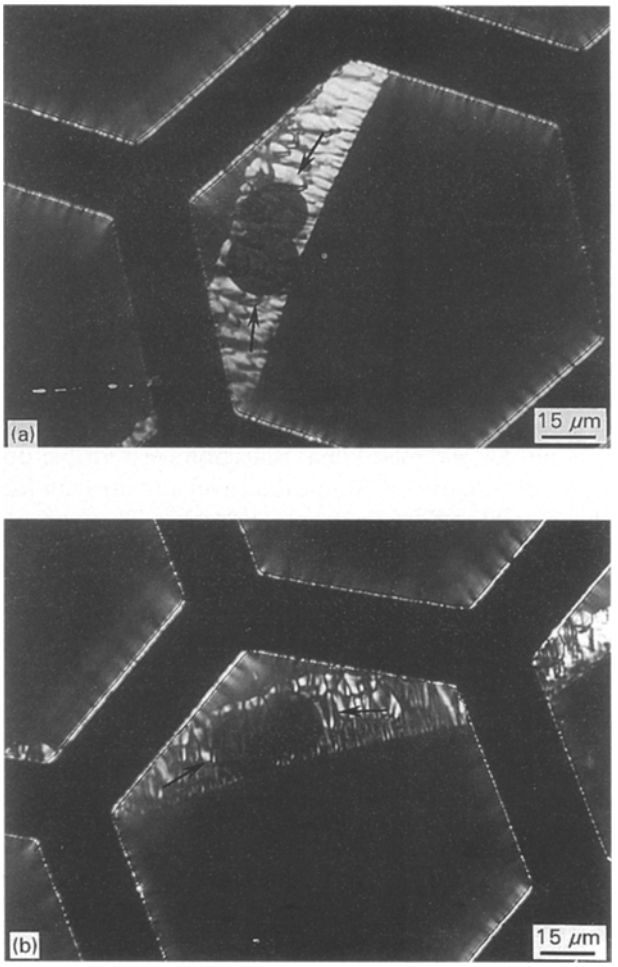


*Figure 4* Polarized optical micrographs showing variations in the birefringence within a film oriented for (a) maximum intensity, and (b) minimum intensity. The areas exposed to the electron beam are evident as circles with the little birefringence (arrowed).

Although the intensity of the strongest reflection fades dramatically upon initial beam exposure, evidence of anisotropy persists for up to 5 min, after which there is no preferential molecular trajectory.

The polypyrrole films considered here are initially quite strongly birefringent when viewed between crossed polars; however, areas exposed to the electron beam subsequently exhibit greatly reduced optical anisotropy. Fig. 4a and b show birefringence within irradiated sections (of a 24 C film), oriented, respectively, for maximum and minimum contrast. The areas exposed to the beam are clearly visible as optically isotropic circles, whose intensity does not change on rotation of the film. Because optical bright-field observations reveal no appreciable changes in optical absorption, this loss of birefringence must result from reduced anisotropy rather than excessive mass loss.

## 3.3. Molecular ordering in polypyrrole

Fig. 5 shows a characteristic nodule (from a 6 C film) observed in dark field, microtome damage is evident as parallel lines crossing the sample. The four insets on the micrograph refer to diffraction patterns from (A, D) nodule-free areas of film and (B, C) two sides of the nodule. The diffraction patterns indicate that,

away from the nodule, the molecules lie parallel to the working electrode, within the nodule the molecules depart slightly from this direction, following a trajectory parallel to the growth surface of the film. Overall, the average molecular orientation within the bulk should be affected only marginally by the growth of the nodules and so X-ray and electron diffraction patterns should be similar, but with a greater degree of randomization in the former case, due to the larger scattering volume (and hence larger range of orientations) that is sampled.

Fig. 6 shows a WAXS pattern collected from a stack of films in cross-section. The pattern consists of two oriented reflections, which lead to $d$ spacings of 0.41 nm for the meridional reflection (just visible on print, but clearly visible on negative) and 0.34 nm for the (clearly visible) equatorial reflection. These are in excellent agreement with the values found from electron diffraction. As expected, the angular spread of both reflections is much greater, indicating a larger range of molecular orientation, compared to electron diffraction. The results confirm that in the bulk there is considerable orientation. In accordance with electron diffraction, the equatorial reflection is the stronger of the two, indicating that the preferential molecular orientation is parallel to the plane of the electrode, the inter-planar stacking distance is 0.33 nm. The weaker meridional reflection corresponds to a less well-defined, planar correlation along the molecular trajectory. In the direction along the chain, 0.41 nm can be taken as the average approach of two pyrrole moieties within the area sampled for the diffraction pattern.

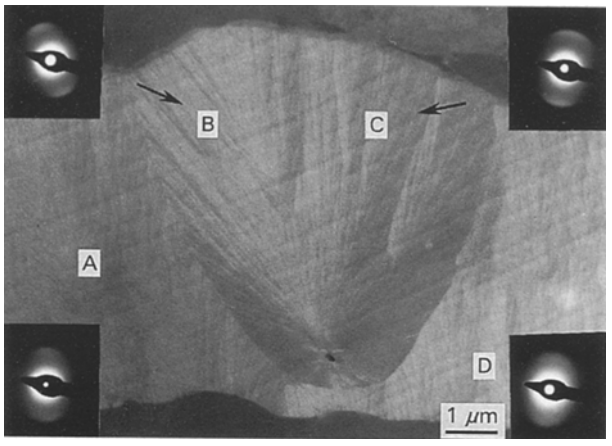


*Figure 5* Dark-field image of a polypyrrole nodule with insets showing the electron diffraction pattern obtained from each of the indicated areas.

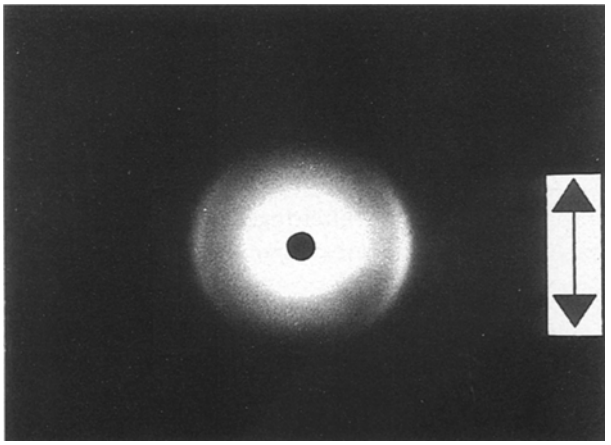

*Figure 6* Wide-angle X-ray scattering pattern taken with the specimen oriented to present the cross-section to the X-ray beam; the arrow indicates the plane of the film.

## 3.4. Compositional variations within the film

Immediately apparent within cross-sections are local variations in contrast, of the type shown in Fig. 7a. Clearly evident within the micrographs are small localized regions of high contrast and a definite streaking from the base of the film towards the growth surface. Because polypyrrole is not crystalline, these dark regions cannot be due to Bragg scattering and it is also unlikely that changes in microtomed thickness could be so localized. Although "Z-contrast" seems to be the most plausible explanation of these features, such spatial variations of counter-ion density have never been reported in polypyrrole. As the conduction process in conducting polymers is strongly associated with the presence of counter ions, any concentration of such species at certain sites in the morphology is likely to have a great bearing on the resulting properties, and a detailed analysis of these features is therefore essential. Slowly scanning the electron beam over the sample and collecting the resultant emitted X-rays should provide a clear picture of compositional variations within the specimen. Usage of such a technique is validated by the previous experiments which show polypyrrole to be stable under such conditions.

Fig. 7b and c show the results of a line scan (X–Y) across the film section of Fig. 7a. Fig. 8a–c show the results of a similar experiment on a single polypyrrole nodule. Both traces are for films grown to 6 C. The beam (spot size 7 nm) was scanned over 125 points on the line and the resultant video trace (intensity) and sulphur count were collected. The video trace shows areas of high intensity at either end of the line scan, where the film section is surrounded by resin and a low intensity in the centre corresponding to the dark region labelled A. The dip in video signal at A is coupled with a rise in the intensity of the sulphur trace; the trace is displayed as an absolute measurement (not to scale), for clarity. As can be seen, the collection of sulphur is very sensitive to the molecular architecture present within the films. The collected count rises sharply upon the beam encountering the film, and closely mirrors the intensity trace. Clearly, the dark area in the centre of the nodule incorporates a much greater density of counter ions than the surrounding film. However, at this stage it is not clear whether the localizations are a consequence of the manner in which these features grow or whether the features grow as a result of localizations of the counter ions. Arguments for each case can be presented. Clearly, however, such a localization will disturb the local

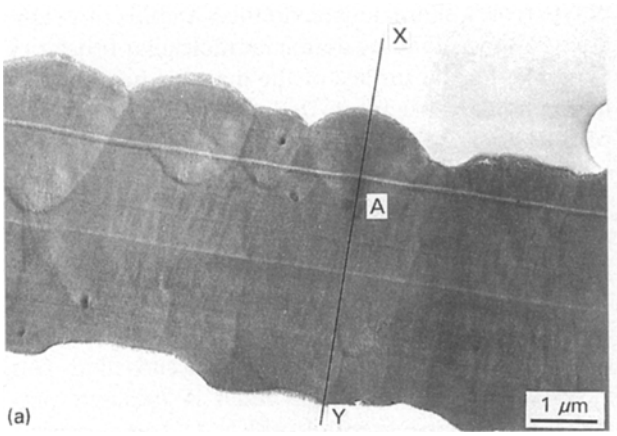


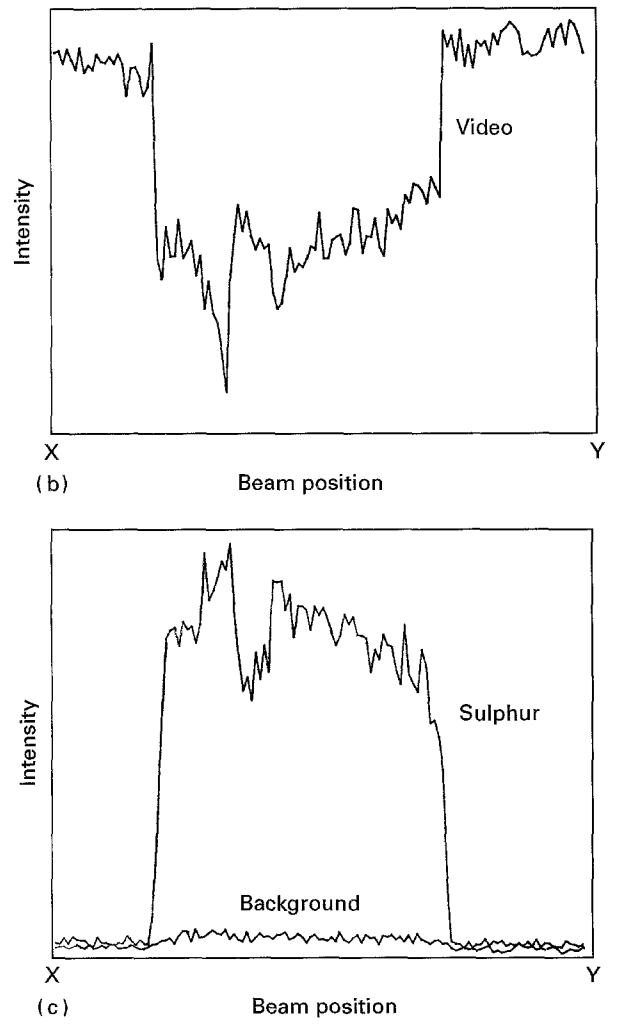


*Figure 7* (a) Transmission electron micrograph, showing the line (X–Y) of scan over the polypyrrole film, including a highlighted high-contrast feature (A); (b) video count from line X–Y; (c) sulphur count\background trace.

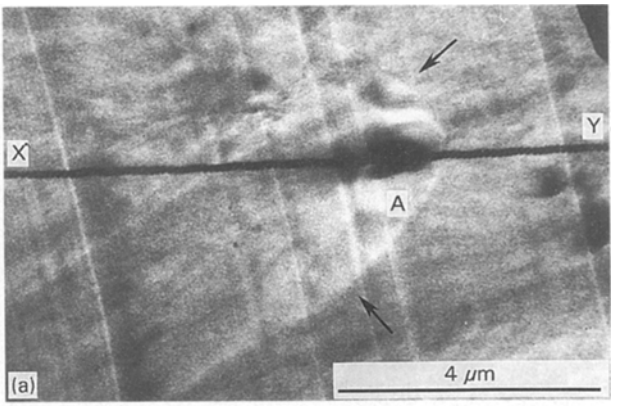


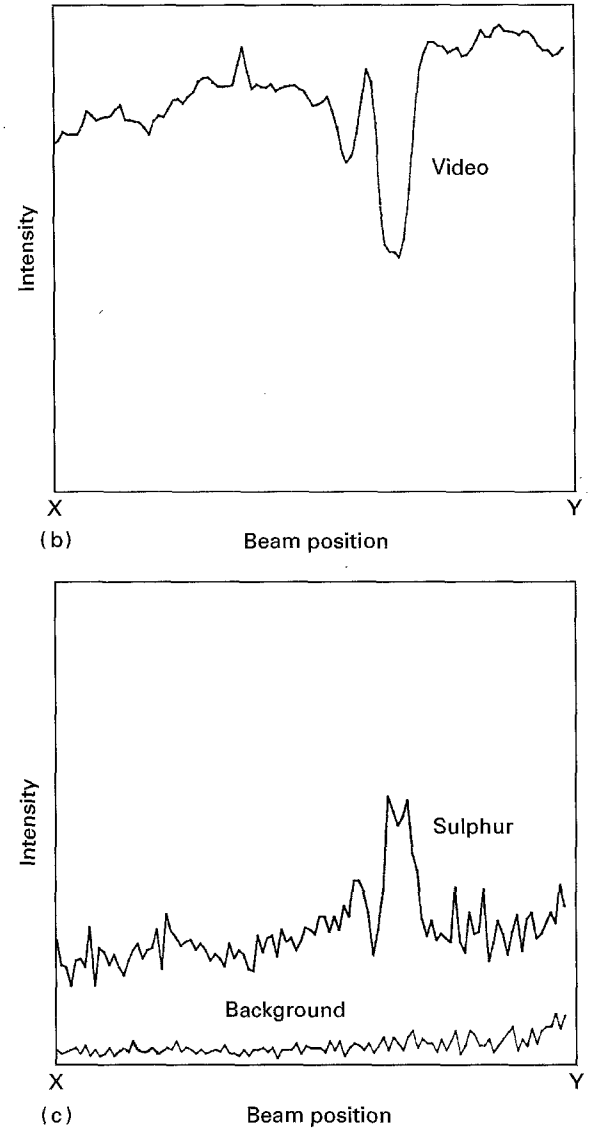


*Figure 8* (a) Detail micrograph, showing the line (X–Y) of scan over a single nodule, including a highlighted (A) dark feature; arrows indicate the nodule boundary. (b) Video count over the line, (c) sulphur count\background trace over the line.

conductivity. Assuming the film cross-section to be presented perpendicular to the cutting edge and that the thickness is 100 nm, then we can estimate the volume of the section of nodule to be 3.04 $\mu m^3$, and the volume of the dark central feature to be 0.035 $\mu m^3$. The line scan illustrates that the count within the central area is twice that of the surrounding film, therefore assuming that the counter-ion content does not vary over the rest of the film then we see that around 3% of the counter ions enclosed within the nodule are resident within this feature which accounts for around 1% of the volume. The conductivity is governed by $\sigma = ne\mu$, where $n$ is the charge carrier density, $e$ is the carrier charge and $\mu$ is the carrier mobility. Assuming that the carrier mobility is constant over the film and that the density of counter ions is directly proportional to the density of charge

carriers, we see that this grouping of counter ions would also represent a localized conductivity increase of the same value. From a point of view of conducting pathways and polaron density, the material is clearly inhomogeneous and within these noted areas, we would expect the conductivity to be correspondingly higher than the bulk value. Such a collection of excess charges would be unstable with respect to Coulombic repulsion, in order to bring the charge density to a level similar to that of the bulk, there must be a degree of positively charged species within the same area. This, therefore, lends credence to Qian's hypothesis [20] that the doping mechanism in polypyrrole is, in fact, accounted for in a similar manner to that found in polyaniline, namely protonation. Qian suggested that protonation leads to conductivity and that the sulphonate ions are merely present in order to preserve charge neutrality. On this basis, the collection of sulphonate ions can be seen as arising from an initial collection of protons, attracting the negatively charged counter ions. The end result, however, will be the same, within this area there would still be a localization of charge carriers and hence a relative conductivity increase. The question nevertheless remains as to what causes this accumulation of charged species.

Figs 7 and 8c also show the collected backgrounds for each trace, with the results plotted relative to the sulphur count. An arbitrary background window was chosen, close to the $SK_\alpha$ line, where the count due to *bremstrahlung* was comparatively high. As can be seen the background does not change significantly, suggesting that there are no significant density/thickness changes within the sample. Such changes, if large enough, would result in corresponding modifications to the background.

## 4. Conclusions

We have investigated the effects of electron-beam interaction with microtomed cross-sections of polypyrrole films using a variety of transmission microscopy techniques. We found no indication of loss of count rate with increasing exposure for a beam defocused so as to irradiate the complete sample cross-section. For a beam focused down to a fine probe, a similar linear response was obtained. Some evidence for degradation with respect to the *bremstrahlung* background was noted but, compared to the fluorescence from the copper grid, no drastic changes were observed. Mass loss in transmission mode is therefore not a factor that is likely to govern the long-term output of characteristic X-rays, and EDS is therefore a valid technique for analysing spatial variations in the composition of polypyrrole. Examination of the changing electron diffraction pattern and the sample birefringence after continued exposure revealed that molecular ordering in the film is totally lost after exposure to the beam for between 5 and 10 min. It can be concluded that, by polymeric standards, polypyrrole is highly stable with respect to mass loss; however, as is generally found in ordered polymeric materials, molecular correlations are readily destroyed.

Electron diffraction and WAXS have been used successfully to reveal the molecular ordering within polypyrrole's characteristic nodular architecture. Diffraction shows that the dominant molecular trajectory is parallel to the surface of the material hence, apart from nodular structures, the molecular trajectory is parallel to the electrode surface. Controlled STEM scanning of the beam coupled with spectroscopic analysis has been used successfully to reveal spatially dependent compositional changes within the nodular morphology of polypyrrole. In particular, the results clearly show localization of the incorporated dopant counter ions within the centre of the nodular structures that are the basic morphological units in such films. This increased density would also result in localized variations in the charge carrier density and a commensurate increase in conductivity. Whether the localizations of counter ions are produced as a result of the formation of the nodules or vice versa, remains to be investigated.


## Acknowledgements

The authors acknowledge the support of the EPSRC for funding the project, and Dr. S. J. Sutton for synthesis of the films. C. D. G. M. thanks Dr J. Janimak for his technical advice on certain aspects of the project.


## References


1. D. C. BASSETT, "Principles of Polymer Morphology" (Cambridge University Press, Cambridge, 1981).
2. M. TSUJI, in "Comprehensive Polymer Science vol 1", edited by C. Booth and C. Price (Pergamon Press, Oxford, 1989) p. 785.
3. D. T. GRUBB, *J. Mater. Sci.* **9** (1974) 1715.
4. D. VESELY and D. FINCH, in "Electron Microscopy and Analysis 1985", edited by G. J. Tatlock (Hilger, Bristol, 1985) p. 7.
5. D. VESELY, A. LOW and M. BEVIS, in "Developments in Electron Microscopy and Analysis", edited by J. A. Venables (Academic Press, London, 1976) p. 333.
6. D. BLOOR, A. P. MONKMAN, G. C. STEVENS, K. M. CHEUNG and S. PUGH, *Mol. Cryst. Liq. Cryst.* **187** (1990) 231.
7. M. OGASAWARA, K. FUNAHASHI, T. DEMURA, T. HAGIWARA and K. IWATA, *Synth. Met.* **14** (1986) 61.
8. Y. LU, J. LI and W. WU, *ibid.* **30** (1989) 87.
9. S. J. SUTTON and A. S. VAUGHAN, *ibid.* **58** (1993) 391.
10. G. R. MITCHELL, F. J. DAVIS and C. H. LEGGE, *ibid.* **26** (1988) 247.
11. S. A. CHEN and S. H. CHEN, *J. Polym. Sci. C Polym. Lett.* **27** (1989) 93.
12. S. J. SUTTON and A. S. VAUGHAN, *J. Mater. Sci.* **28** (1993) 4962.
13. R. H. GEISS, G. B. STREET, W. VOLKSEN and J. ECONOMY, *IBM J. Res. Develop.* **27** (1983) 321.
14. G. R. MITCHELL and A. GERI, *J. Phys. D Appl. Phys.* **20** (1987) 1346.
15. S. J. SUTTON, PhD thesis, University of Reading (1993).
16. A. F. DIAZ, K. K. KANAZAWA and G. P. GARDINI, *J. Chem. Soc. Chem. Commun.* **14** (1979) 635.
17. G. R. MITCHELL, F. J. DAVIS and M. S. KIANI, *Br. Polym. J.* **23** (1990) 157.
18. A. KASSIM, F. J. DAVIS and G. R. MITCHELL, *Synth. Met.* **62** (1994) 62.
19. R. H. GEISS, in "Proceedings of the 38th Annual Meeting of the Electron Microscopy Society of America" (1980) p. 238.
20. R. QIAN, in "Conjugated Polymers and Related Materials", edited by W. R. Salaneck, I. Lundstrom and B. Rånby (Oxford University Press, Oxford, 1993) pp. 161–9.



*Received 1 December 1994*
*and accepted 15 March 1995*